We have seen that such multiplicity can have a significant impact on system performance. It thus appears desirable to study further how to detect such multiplicities, both from process models and from operating data, and to generalize as far as possible the characteristics of processes likely to lead to input multiplicities. The potential benefits include elimination of the possibility of transients such as those illustrated by Figures 10 and 12. In these transients, the existence of input multiplicities has allowed a transition of the process to an undesirable steady state. Such transitions may be very difficult to detect in practice, and may show up only in longer-term economics of the process operation.

NOTATION

A = general square matrix
a_{ij} = partial derivatives, defined by Eq. 33
C_A, C_R, C_S = concentrations of chemical species
c = general controlled variables
c^* = desired value of c; set-point values
c_A, c_R, c_S = normalized concentrations defined by Eq. 27
D = quantity defined by Eq. 46
d = determinant, defined by Eq. 35
E = activation energy
f = function symbol
G = quantity defined by Eq. 43
G_r = diagonal matrix of reset gains, Eq. 4
g = gain ratio, Eq. 43
g_i = reset gain used in ith control loop
k = reaction velocity constant, time units normalized to one typical residence time
k_o = reaction velocity constant at temperature T_o
M = deviation in manipulated variable, Eq. 9
m = general manipulated variables
p = defined by Eq. 28
R = gas law constant
T = absolute temperature
T_o = reference absolute temperature
t = time
tr = trace
u = normalized absolute temperature, T/T_o
$\partial c/\partial m$ = process gain matrix, Eq. 8
$(\partial c/\partial m)_+$ = transformed process gain matrix, Eq. 18
θ = redefined residence time. Eq. 32
μ = interaction matrix, relative gain array, Eq. 19
τ = residence time, normalized to be unity at typical throughout

LITERATURE CITED

Aris, R., "Chemical Reactors and Some Bifurcation Phenomena," *Ann. N.Y. Acad. Sci.*, **1**, 314 (1979).

Aris, R., and N. R. Amundson, "An Analysis of Chemical Reactor Stability and Control—I," *Chem. Eng. Sci.*, **7**, 121 (1958).

Bristol, E. H., "On a New Measure of Interaction for Multivariable Process Control," *IEEE Trans. Auto. Contr.*, **AC-II**, 133 (1966).

Calo, J. M., and H.-C. Chang, "Catastrophe Theory and Chemical Reactors: Exact Uniqueness Criteria for the CSTR, Catalyst Particle, and Packed Bed Reactor," *Chem. Eng. Sci.*, **35**, 264 (1980).

Chang, H.-S., and J. M. Calo, "Exact Criteria for Uniqueness and Multiplicity of an nth Order Chemical Reaction via a Catastrophe Theory Approach," *Chem. Eng. Sci.*, **34**, 285 (1979).

Chang, H.-S., and J. M. Calo, "Errata," *Chem. Eng. Sci.*, **35**, 2377 (1980).

Halmos, P. R., "Finite Dimensional Vector Spaces," D. Van Nostrand Co., NJ, 2nd ed., 105 (1958).

Niederlinski, A., "A Heuristic Approach to the Design of Linear Multivariable Interacting Control Systems," *Automatica*, **7**, 691 (1971).

Uppal, A., Ray, W. H., and A. B. Poore, "On the Dynamics of Continuous Stirred Tank Reactors," *Chem. Eng. Sci.*, **29**, 967 (1974).

Manuscript received October 7, 1980; revision received August 13, and accepted August 31, 1981.

Photo-Assisted Heterogeneous Catalysis with Optical Fibers

Part III: Photoelectrodes

The concept of using optical fibers to distribute light within heterogeneous photo-assisted catalysts is extended to photo-electrochemical cells. The potential drop in a semiconductor photo-electrode is predicted for various types of ohmic electrical contacts, and the optimum contact location is determined. The variation of electrical conductivity with temperature in non-isothermal bundles of semiconductor-coated optical fibers is considered.

R. E. MARINANGELI and D. F. OLLIS

Department of Chemical Engineering, Princeton University, Princeton, NJ 08540

SCOPE

Optical fibers coated with heterogeneous photo-assisted catalyst are a possible scale-up configuration for all such catalysts. Previous papers considered light transport from the fiber to the catalyst (Marinangeli and Ollis, 1977), and heat and mass transport in bundles of such fibers (Marinangeli and Ollis, 1980). In this paper the bundle of coated optical fibers is analyzed as a photo-electrode for photo-electrochemical cells. Appropriate expressions for the position-dependent conductivity and current density in the semiconducting photo-catalyst are developed.

Correspondence concerning this paper should be addressed to D. F. Ollis, who is presently with the Department of Chemical Engineering, University of California, Davis, CA 95616.

0001-1541-82-7144-0945-$2.00.

With these expressions, the local potential gradient in the semiconductor can be evaluated. The optimum location for minimum power loss, or power input, is calculated for an ohmic contact to remove majority carriers to a counter-electrode. These results depend only on the characteristic penetration depth of light into the fiber, ϕ. A similar analysis for the potential distribution may be applied to non-isothermal bundles of semiconductor-coated optical fibers. The radial temperature gradients and resulting non-isotropic conductivity lead to two dimensional potential distributions.

CONCLUSIONS AND SIGNIFICANCE

Photo-electrodes fabricated from semiconductor-coated optical fibers may be useful for large-scale solar energy conversion to electricity and/or to storable fuels such as hydrogen. An important scale-up consideration is minimization of internal potential losses. In this paper the potential loss in a semiconductor-coated optical fiber is determined. An optimum axial location for a single ohmic contact to minimize resistive power losses is

$$\frac{z}{L} = \frac{1}{\phi} \ln \frac{2(1 - e^{-\phi})}{(1 - e^{-2\phi})}.$$

Multiple contacts and continuous conductor contacts for withdrawal of current to the counter-electrode are also considered.

Large-scale use of such photo-electrochemical cells probably would involve bundling the coated fibers together. The same potential drop occurs for an isothermal bundle of coated fibers as for a single-coated fiber provided the average catalyst thickness per fiber remains the same. In a non-isothermal fiber bundle, heating due to light absorption will increase the conductivity (photo-conductivity may increase or decrease depending on the light intensity) and may reduce the potential drop.

INTRODUCTION

In the conversion of light to chemical or electrical energy with semiconducting photo-electrochemical cells, radiant energy incident on a semiconductor electrode generates holes and electrons. In operation, the minority carrier may diffuse to the surface due to bending of the energy bands. The majority carrier will move to the counter-electrode. When the photo-generated holes and electrons are sufficiently anodic and cathodic respectively with reference to a redox couple, the redox reactions will occur at the electrode surfaces. Chemical energy may be stored if the products of an endothermic redox reaction are collected; the photo-electrolysis of water is interesting in this regard. If the redox reactions are simply reversed at the two electrodes so that no net chemical change (storage) occurs, purely electrical energy is obtained. Photo-electrolysis may be considered as a particular application of photo-electrochemical cells; the same principles apply whether predominantly chemical or electrical energy is obtained. The principles of photo-electrochemical cells have been reviewed elsewhere (Albery and Archer, 1976, 1977; Archer, 1975; Bockris and Uosaki, 1977; Gerischer, 1975, 1976: Manassen et al., 1976; Nozik, 1976a; Wrighton et al., 1976c).

Figure 1 illustrates an n-type semiconductor photo-electrode. The band bending occurs because the bulk Fermi levels of the electrolyte and semiconductor must be equal at equilibrium. The electrolyte Fermi level is the equilibrium redox potential of the electrolyte ($E_F = 4.5\,eV + E_{\text{redox vs. SHE}}$). Consequently, the positions of the semiconductor Fermi level and bulk bands are shifted. The conduction and valence bands are pinned at the surface to their original values, however (Morrison, 1977). The bands are bent in a depletion layer of about 10 to 1,000 nm. For an unbiased n-type semiconductor, the potential curvature drives hole migration to the surface, and the electron is removed to the counter-electrode. When (a) the hole energy (given by $E_v + V_b$) is less than the oxidation potential, *and* (b) the electron energy (given by E_F) is greater than the reduction potential, the redox reaction will proceed. Additional potential may be supplied to the semiconductor from an external bias in order to satisfy these energy requirements.

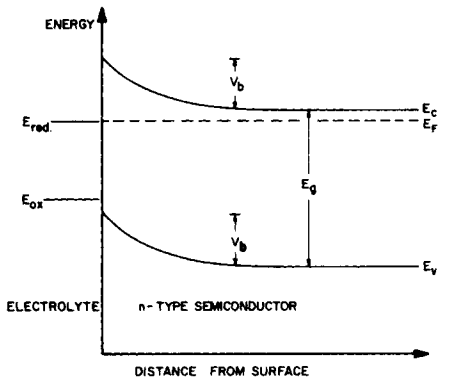

Figure 1. Bending of the energy bands at the semiconductor-electrolyte interface; the equilibrium case.

The most frequently studied photo-electrode materials are listed in Table 1. Many papers have been published on this subject in the last five years, suggesting the proximity of practical application of photo-electrochemical solar energy conversion.

A previous discussion of light transport in a coated optical fiber (Marinangeli and Ollis, 1977) suggested that such a configuration (Figure 2) was potentially useful for scale-up of all reported photoassisted heterogeneous catalysts, including photo-assisted electrolysis. The essential feature of the coated fiber design is that light enters the end of the optical fiber and is repeatedly internally reflected at the semiconductor-fiber interface. At each reflection, a small portion of the light is absorbed by the semiconductor (catalyst) coating. The resulting minority carriers may drive a reaction at the semiconductor-liquid interface, for example, electrolysis of water.

We expect that the fibers may be bundled together into macroscopic arrays for practical applications. The small diameter (10–100 μm) of commercially available fibers insures a large ratio of light transfer surface area to reactor volume. A second study

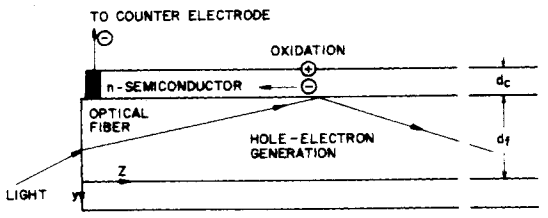

Figure 2. Semiconductor-coated optical fiber.

TABLE 1. SEMICONDUCTOR PHOTO-ELECTRODES

Material	Band Gap(eV)	References
TiO_2	3.0	Carey and Oliver, 1976; Fleischauer and Allen, 1976; Frank and Bard, 1975; Fujishima and Honda, 1973; Fujishima et al., 1975; Gissler et al., 1976; Hardee and Bard, 1975, 1977; Harris and Wilson, 1976; Keeney et al., 1975; Kohl et al., 1977; Laser and Bard, 1976; Mavroides et al., 1975; Morisaki et al., 1976; Nozik, 1975, 1976b; Ohnishi et al., 1975; Ohashi et al., 1977; Wrighton et al., 1975; Yoneyama et al., 1975; Harris et al., 1977; Nozik, 1977; Spitler and Calvin, 1977
$SrTiO_3$	3.2	Mavroides et al., 1976; Ohasi et al., 1977; Wrighton et al., 1976b
CdS	2.4	Chai and Anderson, 1975; Ellis et al., 1976a,c, 1977a; Gerischer, 1975; Kohl et al., 1977; Miller and Heller,1976; Heller et al., 1977; Inoue et al., 1977; Nozik, 1977; Owen, 1977
CdSe	1.7	Ellis et al., 1976a,c, 1977a; Gerischer, 1975; Hodes et al., 1976; Manassen et al, 1977; Heller et al., 1977; Owen, 1977
CdTe	1.5	Ellis et al., 1976b, 1977a; Ohashi et al., 1977
GaP	2.3	Gerischer, 1977; Kohl et al., 1977; Nakato et al., 1975, 1976; Nozik, 1976; Ohashi et al., 1977; Tomkiewicz and Woodall, 1977; Yoneyama et al., 1975; Ellis et al., 1977b; Nozik, 1977
GaAs	1.5	Chai and Anderson, 1975; Ellis et al., 1977b; Gourgaud and Elliot, 1977; Kohl et al., 1977; Chang et al., 1977
WO_3	2.7	Butler et al., 1976; Hardee and Bard, 1977; Hodes et al., 1976; Butler, 1977
ZnO	3.2	Fujishima et al., 1976; Gerischer and Camman, 1972
SnO_2	3.5	Kim and Laitinen, 1975; Wrighton et al., 1976a
Si	1.1	Candea et al., 1976; Kohl et al., 1977; Nakato et al., 1975; Jayadevaiah, 1974
Fe_2O_3	2.2	Hardee and Bard, 1977; Quinn et al., 1976; Yeh and Hackerman, 1977
$KTaO_3$	3.4	Ellis et al., 1976d
Bi_2O_3	2.8	Hardee and Bard, 1977
CuO	1.7	Hardee and Bard, 1977
InP	1.3	Kohl et al., 1977
Bi_2S_3	1.3–1.4	Miller and Heller, 1976
$BaTiO_3$	3.3	Nasby and Quinn, 1976
$Pb_{0.86}La_{0.14}(Zr_{0.10}Ti_{0.90})_{0.965}O_3$3.0 (PLZT)		Nasby and Quinn, 1976
$Pb_{0.92}La_{0.08}Ti_{0.98}O_3$ (PLT)	2.9	Nasby and Quinn, 1976
$FeTiO_3$, Fe_2TiO_4, Fe_2TiO_5 2.1–2.2MoS_2	1.7–1.8	Ginley and Butler, 1977 Tributsch, 1977

considered heat and mass transport in layers of photo-assisted heterogeneous catalysts coated on optical fibers and in bundles of coated fibers (Marinangeli and Ollis, 1980). The present paper analyzes the influence of bulk electron (hole) transport when catalyst coated fibers are used as photo-electrodes.

PHOTO-ELECTRODE APPLICATIONS

This paper considers the application of the coated optical fiber concept to photo-electrochemical cells. Photo-electrochemistry with coated optical fiber electrodes will require the following events to occur (Figure 2):

(a) Light entering one end of the optical fiber (light pore) is "piped" down the fiber by internal reflection at the catalyst fiber interface.

(b) At each reflection, due to surface scattering and absorption of the evanescent wave, the intensity propagated down the fiber diminishes (exponentially in an isothermal system).

(c) The absorbed light drives the photo-electrochemical half-cell reaction of the electrode, and

(d) simultaneously heats the semiconductor.

(e) The majority carriers created in the above reaction are transported, via conduction, to the counter-electrode. Events (a), (b) and (d) have been considered previously (Marinangeli and Ollis, 1977, 1980). This discussion focuses on (c) and (e).

The axial light intensity in the fiber, I_a, is related to the light intensity in the semiconductor at the semiconductor-fiber interface, I_{oc}, by a factor β_c (or β_c' or β_c'').

$$I_{oc} = \beta_c I_a$$

The factor β_c is a function of the incident angle of the internally reflected light and the relative refractive indices of the media involved (Marinangeli and Ollis, 1977; Harrick, 1967).

Control of the intensity, and thereby the electrochemical rate is important for several reasons. First, the quantum yield (number of carriers in the external circuit per incident photon) often decreases with increasing light intensity (Carey and Oliver, 1976). [The quantum yield is the same as the photo-conductive gain (Bube, 1960). The use of the term photo-conductive gain is especially appropriate when an external bias voltage is applied to increase the quantum yield (gain).] Thus, photons may be used more efficiently at lower local absorption rates. In addition, an electrode overpotential is minimized for slower electrochemical rates per unit catalyst area. Reduction of the local over potential increases the energy efficiency of photo-electrochemical cells (Nozik, 1975; Manassen et al., 1976). Finally, quenching of the semiconductor dissolution as in, e.g., cadmium sulfide or cadmium selenide electrodes by polysulfide electrolyte, might be mass transfer limited at high light intensities or high electrochemical rates (Ellis et al., 1976c). Moderation of the rate would allow the dissolution to be quenched by lower concentrations of polysulfide.

Light supplied to a photo-electrode by optical fibers will not pass through most of the bulk reactant-product phase. This may be

advantageous in two cases. When a gaseous product is formed from a liquid reactant, as with hydrogen and/or oxygen from water, bubbles may be generated when the liquid becomes supersaturated. These bubbles will scatter some of the incident light away from the photo-catalyst. Also, some electrolytes, including polysulfide and ditelluride solutions, absorb light. In either case, use of optical fibers to supply light will reduce light loss in the bulk electrolyte.

A photoelectrode of appreciable semiconductor-electrolyte interfacial area arises from coating the fiber with a porous semiconductor layer formed by sintering a deposited semiconductor powder. Such a porous structure would allow a semiconductor-electrolyte interface to exist throughout the coating. The disorder in the sintered regions joining the semiconductor particles would reduce carrier mobility, but might also generate numerous donor or acceptor states. Consequently, the conductivity will depend on the preparation technique.

We may anticipate that a central problem with using thin semiconducting layers coated on the walls of optical fibers is the resultant potential loss for transport of electrons (or holes) to the counter electrode. A simple energy balance on a photo-electrochemical cell (Nozik, 1975, 1976a) shows that

$$E_g - V_B - (E_c - E_F) = \frac{\Delta G}{nF} + \eta_a + \eta_c + ir + v_H$$

when $\Delta G/nF$ is the free energy per electron for the cell reaction, η_a and η_c are the anodic and cathodic overpotentials respectively, ir is the ohmic loss and V_H is the potential drop across the Helmholtz layers in the electrolyte (Figure 1). This balance shows that ohmic loss must be subtracted from the available photo-electrochemical energy (terms on the left hand side of the equation). Obviously, the design of the photo-electrochemical cell must minimize internal losses.

In this paper we examine how the ohmic losses vary with the parameters of a coated optical fiber photo-electrode. As such losses depend, inter alia, on external junction (contact) location, several junction locations will be evaluated. First, some of the general features of transport in thin films of amorphous semiconductors must be considered as these are expected to resemble the semiconductor coatings envisaged above.

ELECTRON TRANSPORT IN AMORPHOUS SEMICONDUCTORS

Although amorphous semiconductors lack the long range order which give sharp energy bands for crystalline solids, the energy band concept is still valid (Adler, 1971; Grigorovici, 1971; Hill, 1972). Structural disorder causes a smearing of the sharp energy band edges of crystals with consequent formation of tails of states in the energy gap. In some instances, the band tails may overlap. Consequently it appears to be more realistic to consider a carrier (electron or hole) mobility gap, that is a range of energies in which electrons (or holes) have negligible mobility, rather than an energy band gap. Nevertheless, Ohm's law is usually valid for low fields. (Only for very low temperatures or very high concentrations of defect levels in the gap, will a hopping mechanism, that is tunneling between localized states, be responsible for conduction.)

Ohm's law states (Kittel, 1971)

$$\vec{j} = \sigma \vec{E}$$

where $\vec{j}$ is the current density, σ is the conductivity and $\vec{E}$ is the electric field. The conductivity for a semiconductor is

$$\sigma = (ne\mu_e + pe\mu_h)$$

where e is the electrical charge; n and p are the concentrations of conduction band electrons and valence band holes respectively; and μ_c and μ_n are the mobilities of these holes and electrons respectively. For a photo-electrode, the minority carriers may be consumed by electrochemical reaction near their site of generation or by recombination with a majority carrier. For simplicity, we consider the most typical photoelectrode: an n-type semiconductor. Here, we will consider only the transport of the photo-generated majority carriers.

The mobility is the magnitude of the drift velocity per unit electric field, expressed as

$$\mu = \frac{e\tau}{m_e}$$

where τ is a collision time and m_e is the effective mass of an electron. The collision time may be related to a characteristic collision distance or electron mean free path ℓ by

$$\ell = v_{th}\tau$$

where v_{th} is the electron thermal velocity.

The collision length in the bulk is related to the frequency of defects or disorder in the semiconductor crystal. Obviously, amorphous semiconductors contain much disorder and have relatively short collision distances, hence are typified by low mobilities. The mobility can be increased significantly by annealing to decrease the disorder. In thin films, the mean free path ℓ can be reduced further by collisions with the free surface (Chopra, 1969) (here, the solid-electrolyte interface). In the simplest case, the thin film mobility, μ_F, is related to the bulk mobility, μ_B, by

$$\mu_F = \frac{\mu_B}{1 + \ell/t}$$

where t is the film thickness. Note that mobility and conductivity are averaged transport properties since, like molecular diffusion, they are meaningful over a region necessarily larger than the appropriate mean free path.

The current density, $\vec{j} = ne\vec{v}_e$, where $\vec{v}_e$ is an electron velocity, and the conductivity, $\sigma = ne\mu_e$, each depend on the concentration of conduction electrons. Carrier concentrations in semiconductors are typically low, since they arise from thermal excitation across the band gap (intrinsic carriers) and impurity doping (extrinsic carriers). In photoelectrodes, however, additional carriers will be generated by photons. Thus the current and conductivity will each depend on the light intensity and will be larger than the corresponding thermal values.

CALCULATION OF THE POTENTIAL LOSS

The internal axial potential gradient for a semiconductor photoelectrode coated on an optical fiber (Figure 2) is given by Ohm's law in differential form:

$$\frac{dV}{dz} = -\frac{1}{\sigma(z)} j(z) \tag{1}$$

First, expressions for the position dependent current and conductivity must be determined. Then $(dV/dz)dz$ may be evaluated for the appropriate current path in order to determine the potential loss. Note that Ohm's law behavior is observed for both amorphous semiconductors (Grigorivici, 1971) and semiconductor particles of sufficiently small size, such as less than 0.1 μm (Mark and Sang Lee, 1974).

For the semiconductor coated optical fiber, in the annular catalyst layer both the current density and the potential will be functions of axial position, and a reactant, light, has an axially dependent magnitude. The current density at z is obtained by a summation of the photo-generated electron (hole) flux and division by the axial cross sectional area of the coating. The potential distribution is obtained from Ohm's law, using the previously determined light intensity profile (Marinangeli and Ollis, 1977). The radial flux of liquid electrolyte should be insignificant; the potential loss will occur in axial majority carrier transport.

We first assume that the single fiber is isothermal. A previous paper (Marinangeli and Ollis, 1980) showed that the heating due to light absorption is insignificant for single fibers coated with catalyst. For photo-electrode applications, resistive heating also occurs. In the absence of an external bias, the energy for resistive heating is supplied by the incident photons. Hence, resistive heating cannot exceed heating which occurs if all of the incident photons

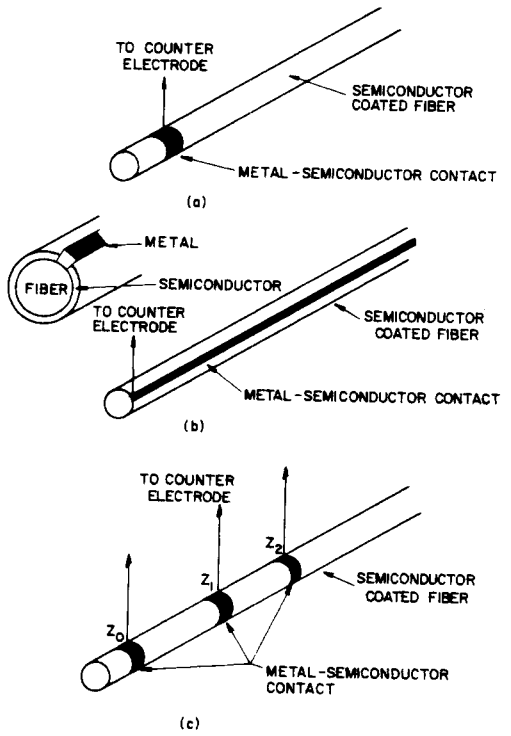

Figure 3. Metal-semiconductor contacts for withdrawal of majority carriers to the counter-electrode: a) a single contact, b) a continuous contact, and c) a series of contacts.

are converted directly to thermal energy.

Consider a semiconductor film of length L and thickness d_c coated on an optical fiber of diameter d_f (Figure 2). The total current generated by light absorption, J, in the length z_1 and z_2 is

$$J = \int_{z_1}^{z_2} \int_0^{d_c} \alpha_c I_c \chi \pi d_f dz dy \tag{2}$$

where α_c is the absorption coefficient, I_c is the light intensity in number of photons per area per time, and χ is the quantum yield. We will use the convention that a current of electrons (negative charge) in the direction L to z (negative) is positive. The integration is taken over a thin (slab) annulus, a valid assumption when integrating the evanescent light intensity (for which $d_p \ll d_f$) (Marinangeli and Ollis, 1977). Division by the semiconductor annular area, $\pi d_f d_c$, yields the current density at z.

$$j(z) = \frac{\alpha_c \chi}{d_c} \int_{z_1}^{z_2} \int_0^{d_c} I_c dy dz \tag{3}$$

An appropriate form for the conductivity is

$$\sigma(z) = \sigma_0 + \sigma_p(z), \tag{4}$$

where the photo-conductivity $\sigma_p(z)$ is taken as the *increase* in conductivity due to incident radiation (Kittel, 1971). The position-independent part of the conductivity, σ_o, is the intrinsic conductivity. The photo-conductivity, $\sigma_p(z)$, depends on the light intensity and therefore is position-dependent. The photo-conductivity for amorphous semiconductors is directly proportional to the rate of photon absorption for moderate carrier generation rates, where electron trapping is the principal recombination route. At higher absorption (carrier generation) rates, hole-electron recombination becomes significant and the photo-conductivity tends towards a square root dependence on carrier generation (Kittel, 1971; Taylor and Simmons, 1972; Simmons and Taylor, 1972). At such high generation rates (light intensities), hole-electron recombination will also decrease the quantum efficiency of the semiconductor photo-electrode. We will be primarily concerned with the linear region of the photo-conductivity-light intensity dependence, that is the high quantum yield region. If we assume that the effect of the light intensity is to increase the conduction band electron concentration from its intrinsic value, n_o, to a new concentration equal to the number of photons absorbed divided by the recombination rate due to trapping, R', (Kittel, 1971) the expression for the photo-conductivity in a differential volume dv is

$$\sigma_p(z) = \frac{\alpha_o}{n_o} \frac{\alpha_c I_c dv}{r' dv}. \tag{5}$$

Recall that for this application we need only consider the concentration of the majority carriers since the minority carriers are not transported through the photoelectrode, but are removed instead by the half cell reaction at the local surfaces.

Both the current density and the conductivity depend on the light intensity.

We hve shown (Marinangeli and Ollis, 1977) that the appropriate form for the evanescent light intensity is

$$I_c = \beta_c I_o \exp\left(-\frac{z\phi}{L} - \frac{2y}{d_p}\right). \tag{6}$$

[If most of the light is supplied to the semiconductor by scattering at the fiber-semiconductor interface, a similar exponential expression for the light intensity is correct (Marinangeli and Ollis, 1977). In this paper we will use the light intensity for the evanescent wave only.]

ELECTRICAL CONTACT AT THE FIBER END

With the contact made at the most intensely illuminated end of the fiber (Figure 3a), the current flux at any point z is given by Eq. 7.

$$j(z) = \frac{\alpha_c \chi}{d_c} \int_z^L \int_0^{d_c} I_c dy dz \tag{7}$$

The conductivity in a segment dz is given by

$$\sigma = \sigma_o + \frac{\sigma_o \alpha_c}{n_o d_c R'} \frac{\int_0^{d_c} I_c dy (\pi d_f dz)}{(\pi d_f dz)} \tag{8}$$

In each case the light intensity in the semiconductor is given by Eq. 6. Performing the integration yields

$$j(z) = \frac{\alpha_c \beta_c I_o \chi d_p}{2 d_c} \frac{L}{\phi} (1 - e^{2d_c/d_p})(e^{-z\phi/L} - e^{-\phi}) \tag{9}$$

and

$$\sigma = \sigma_o + \frac{\sigma_o \alpha_c \beta_c I_o d_p}{2 n_o R' d_c} (1 - e^{2d_c/d_p}) e^{-z\phi/L}. \tag{10}$$

Substitution of these expressions into Ohm's law (Eq. 1) yields

$$\frac{dV}{dz} = \frac{Be^{-\phi} - Be^{-z\phi/L}}{C + De^{-z\phi/L}} \tag{11}$$

where

$$B = \frac{\alpha_c \beta_c I_o \chi d_p}{2 d_c} \frac{L}{\phi} (1 - e^{2d_c/d_p})$$

$$C = \sigma_o$$

$$D = \frac{\sigma_o \alpha_c \beta_c I_o d_p}{2 n_o R' d_c} (1 - e^{2d_c/d_p}).$$

The total potential drop in the semiconductor film is

$$V = \int_0^L \left(\frac{dv}{dz}\right) dz$$

$$= \frac{LB}{\phi} \left[\frac{e^{-\phi}}{C} \ln\left(\frac{Ce^{\phi} + D}{C + D}\right) - \frac{1}{D} \ln\left(\frac{C + D}{C + De^{-\phi}}\right)\right]. \tag{12}$$

Relative plots of the light intensity (or photoconductivity or local reaction rate), the current density, and the potential are shown in Figure 4.

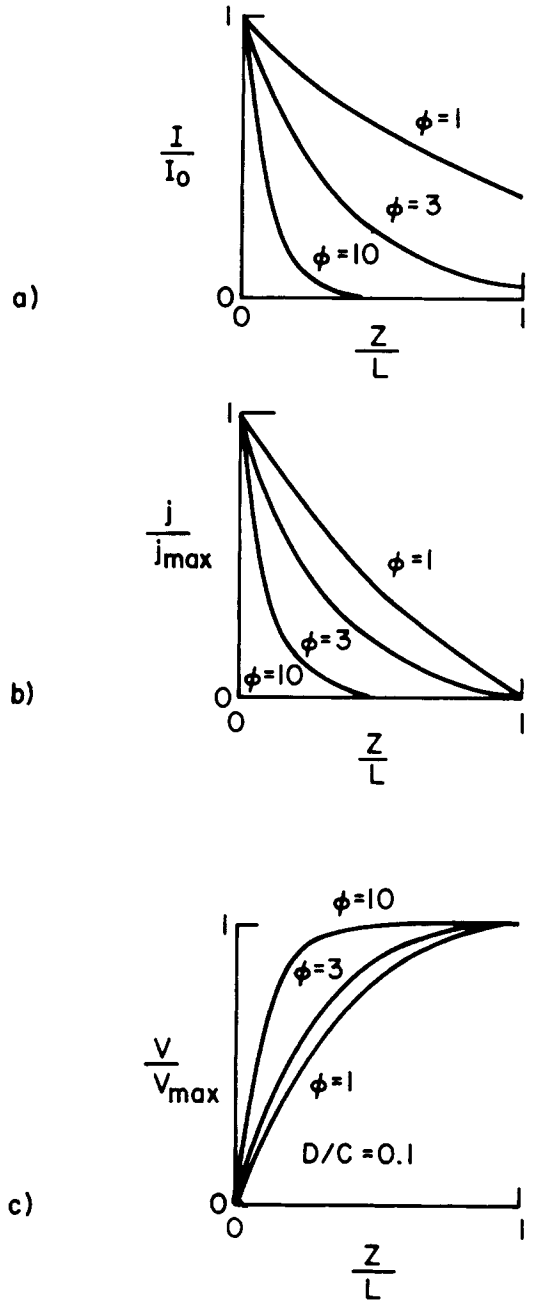

Figure 4. Relative plots of a) light intensity (or photo-conductivity or reaction rate), b) current density, and c) potential, for a coated fiber with an ohmic contact at the end.

ARBITRARY CONTACT LOCATION

Suppose the electrical contact is located at an arbitrary position, z^*, between 0 and L. The solution for the segment from z^* to L is similar to the result obtained for the contact at one end. The final integration is from z^* to L rather than 0 to L. The result is

$$V_{z^*-L} = \frac{LB}{\phi}\left[\frac{e^{-\phi}}{C}\ln\left(\frac{Ce^{\phi}+D}{Cu+D}\right) - \frac{1}{D}\ln\left(\frac{C+Du^{-1}}{C+De^{-\phi}}\right)\right] \quad (13)$$

where $u = \exp(z^*\phi/L)$.

For the segment from 0 to z^* the current density expression including the direction change of the current flow is

$$j_{0-z^*}(z) = -\frac{a_c\chi}{d_c}\int_0^{z^*}\int_0^{d_c} I_c dy dz = \frac{\alpha_c\chi\beta_c I_o d_p}{2d_c}\frac{L}{\phi}(1-e^{2d_c/d_p})(e^{z\phi/L}-1). \quad (14)$$

The potential change from z^* to 0 is

$$V_{0-z^*} = \frac{LB}{\phi}\left[\frac{1}{C}\ln\left(\frac{C+D}{Cu+D}\right) + \frac{1}{D}\ln\left(\frac{C+D}{C+Du^{-1}}\right)\right].$$

OPTIMUM CONTACT LOCATION

Part of the electrochemical energy generated in the photo-electrode will be dissipated internally by resistive heating. This power loss can be minimized by proper choice of the contact location. In differential form, the power consumed by resistive heating is

$$P = \int_{z_1}^{z_2} -j(z)a\left(\frac{dV}{dz}\right)dz \quad (15)$$

or, using Ohm's law,

$$P = \int_{z_1}^{z_2}\frac{j(z)^2 a}{\sigma(z)}dz. \quad (16)$$

For a semiconductor photo-electrode with an ohmic contact at z^* the total power dissipated is the sum of the power dissipated in each segment.

$$P = \int_0^{z^*}\frac{j_{0-z}(z)^2 a}{\sigma}dz + \int_{z^*}^{L}\frac{j_{L-z}(z)^2 a}{\sigma}dz \quad (17)$$

The optimum contact location for minimum power dissipation is obtained from

$$\frac{dP}{dz^*} = \frac{j_{0-z^*}(z^*)^2 a}{\sigma(z^*)} - \frac{j_{z^*-L}(z^*)^2 a}{\sigma(z^*)} = 0. \quad (18)$$

The value z^* thus satisfies the relation

$$j^2_{0-z^*}(z^*) = j^2_{z^*-L}(z^*), \quad (19)$$

Use of Eqs. 14 and 9 gives

$$\frac{z^*}{L} = \frac{1}{\phi}\ln\frac{2(1-e^{-\phi})}{(1-e^{-2\phi})}. \quad (20a)$$

The asymptotic values are

$$\frac{z^*}{L} = \frac{\ln 2}{\phi} \text{ as } \phi \to \infty \quad (20b)$$

$$\frac{z^*}{L} = 1/2 \text{ as } \phi \to 0. \quad (20c)$$

ALTERNATE CONTACT CONFIGURATIONS

We have thus far considered only a single point contact to the semiconductor photo-electrode. Several other possibilities exist. If the conductivity of the illuminated semiconductor is too low to allow a single end contact, a continuous metal wire or strip could be imbedded in the semiconductor or on either surface of the semiconductor along the axis of the fiber (Figure 3b). This configuration might be especially attractive if the fibers are bundled together. High conductivity wires, acting as contacts, could be interspersed with the fibers. [SnO_2 coatings are often used to make conducting transparent coatings. SnO_2 is transparent to visible light ($Eg = 3.5\ eV$) and has a relatively high conductivity for a semiconductor. SnO_2 coated optical fibers could be used to supply light and remove current. The SnO_2 coating would be equivalent to an embedded wire.] Since the conductivity of the metal contact (typically $10^6\Omega^{-1}\text{cm}^{-1}$) is much greater than that of the annular semiconductor (10^2 to $10^{-9}\Omega^{-1}\text{cm}^{-1}$), the axial conductivity becomes simply

$$\sigma = \sigma_o(\text{metal})$$

and the appropriate cross-sectional area for current flow is the cross-sectional area of the wire. Obviously the axial potential drop should be negligible unless the wire cross-sectional area is very small.

In addition, there will be a radial potential drop in the semi-

TABLE 2. PARAMETERS FOR POTENTIAL DROP CALCULATIONS

$\alpha_c = 10^4\ \text{cm}^{-1}$

$\chi = 0.1$

$\beta_c = 0.1$

$I_o = 2 \times 10^{-3} \dfrac{\text{mol}}{\text{s} \cdot \text{m2}}$

$d_p = 400\ \text{nm}$

$\mu_e = 210 \dfrac{\text{cm}^2}{\text{V} \cdot \text{s}}$

conductor around the annular fiber coating. This potential drop may be calculated between the contact wire and the opposite side of the fiber, a distance of $\pi d_f/2$. Modelling the annual layer as a slab πd_f along with the contact at the origin (Figure 5) yields

$$V = \frac{-\dfrac{B\phi(\pi d_f)^2}{8L} e^{-z\phi/L}}{C + De^{-z\phi/L}}. \qquad (21)$$

Of course the voltage drop depends on z because of the dependence of the radial current and the conductivity on the light intensity.

A series of contacts located at positions $z_0, z_1, z_2 \ldots z_n$ may be used (Figure 3c). The potential loss in each segment consists of two parts. Current in the length z_m to z' will flow to z_m and current in the length z' to z_{m+1} will flow to z_{m+1} where z' is the equipotential point between z_m and z_{m+1} (i.e., value of z' satisfying

$$\int_{z'}^{z_m} \left(\frac{dV}{dz}\right) dz = \int_{z'}^{z_{m+1}} \left(\frac{dV}{dz}\right) dz.$$

The lengths will be unequal due to the axially diminishing light intensity. The values of dV/dz may be obtained as for the case of an arbitrary contact location.

NUMERICAL EXAMPLES

The potential loss for a semiconductor-coated optical fiber with an ohmic contact at $z = 0$ was calculated using the parameters in Table 2. These values might be typical of *CdS* illuminated by sunlight. The fiber diameter, fiber length, and catalyst thickness were varied. The potential drop was calculated for various values of the intrinsic conductivity and recombination rate. The intrinsic electron concentration was calculated from the relationship $\sigma = n_o e/\mu_e$.

Table 3 shows calculated potential drops for various catalyst thicknesses on a 0.1 m long optical fiber with a 200 μm diameter. The conductivity is $100\Omega^{-1}\text{cm}^{-1}$ which is high for a semiconductor. (Values for semiconductor photo-electrodes are reported in Table 4.) The following features are apparent. First, $\phi \geq 1$ for thin semiconductor (catalyst) films even for this short fiber. Thus, all of the light can be absorbed in a short fiber. Next, large potential losses in thin films ($d_c < 500$Å) can occur even for very high conductivity. The potential loss is negligible only when all of the light is absorbed near the entrance (ϕ is large, e.g., $d_c > 500$ nm for Table 3 example). Finally, a large change in the recombination rate produced only a small change in the potential loss. The difference decreases as ϕ increases since most of the light is absorbed very near

TABLE 3. CALCULATED POTENTIAL DROP

$\sigma_o = 100\ \Omega^{-1}\ \text{cm}^{-1}$

$d_f = 200\ \mu\text{m}$

$L = 0.1$ m

d_c (nm)	ϕ	V ($R' = 2 \times 10^{11}\ \text{s}^{-1}$)	V ($R' = 1 \times 10^{8}\ \text{s}^{-1}$)
5	0.987	-5.07	-1.87
15.8	3.04	-1.62	-1.62
50	8.85	-2.17×10^{-1}	-1.69×10^{-1}
158	21.85	-2.79×10^{-2}	-1.85×10^{-2}
500	36.71	-5.25×10^{-3}	-3.28×10^{-3}
1,580	39.98	-1.53×10^{-3}	-1.53×10^{-3}
5,000	39.99	-4.82×10^{-4}	-4.82×10^{-4}
15,800	39.99	-1.52×10^{-4}	-1.52×10^{-4}

TABLE 4. PHOTO-ELECTRODE CONDUCTIVITIES

Material*	Conductivity ($\Omega^{-1}\ \text{cm}^{-1}$)	Reference
TiO_2	0.3	Nozik, 1975, 1977
TiO_2**	0.1-1.	Morisaki et al., 1976
CdS	0.166-0.5	Ellis et al., 1976c, 1977a
	2.	Nozik, 1977
CdSe	0.07-10.	Ellis et al., 1976c, 1977a
GaP	1.-3.7	Ellis et al., 1977b
	3.-10.	Nozik, 1977
GaAs (Si or Te Doped)	333.-1.000.	Ellis et al., 1977b
WO_3	0.001	Butler et al., 1976
$SrTiO_3$	0.07	Mavroides et al., 1976
$BaTiO_3$	0.55	Nasby and Quinn, 1976
$FeTiO_3$, Fe_2TiO_4, Fe_2TiO_5	0.01-0.001	Ginley and Butler, 1977
Fe_2O_3	0.003	Quinn et al., 1976
SnO_2 (Sb Doped)	10.	Wrighton et al., 1976
MoS_2 (I_c)	0.1-1.	Tributsch, 1977

* Single crystals except where indicated.
** Chemically vapor-deposited amorphous material.

the fiber end and the resulting length scale for electron transport is very small. The reason for the relatively small change in voltage drop with R' is that for the larger R' (probably a more realistic value) the photoconductivity is negligible. For the smaller R', the photoconductivity is still small in comparison to the intrinsic conductivity.

These calculations suggest that short optical fibers clad with thin layers of a semiconductor might be useful photoelectrodes, but it may be necessary to embed an axial metallic conductor in the photoelectrode to reduce the internal potential drop. A small *continuous* semiconductor coating would be required to avoid metal-electrolyte short circuit.

A similar calculation for the radial potential drop around a fiber with $\sigma_o = 0.5\ \Omega^{-1}\text{cm}^{-1}$, $d_c = 500$ nm and $d_f = 200\ \mu$m showed that the maximum radial potential drop ($z = 0$) was negligible (1.5×10^{-3} V).

THE FIBER BUNDLE

In a previous paper, we pointed out that a bundle of catalyst coated optical fibers would be a reasonable large scale configuration. This compact arrangement would allow contacting of a large catalyst surface area within a relatively small volume. Three possibilities are envisioned. Separate single fibers could be bound together externally (Figure 6a), fibers could be embedded in a continuous semiporous semiconductor (Figure 6b) or attached to a planar metallic sheet (Figure 6c). In the latter cases, the porosity required for electrolyte supply will diminish the conductivity very markedly (due to reduction of the electron mean free path) unless the semiconductor is sufficiently annealed. In this case, it is likely that conducting wires would be embedded in the semiconductor between the fibers.

Our previous analysis of axial carrier transport in coated single fibers applies equally well for an isothermal fiber bundle, provided that the ohmic contact is effective at each fiber in the bundle. Thus the expression for the position-dependent current flux remains the same, and the axial cross section of catalyst fiber is that of Figure

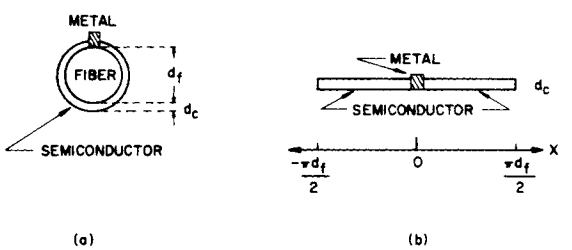

Figure 5. Angular potential drop around a fiber: a) end view of coated fiber, b) slab approximation of semiconductor, "unwrapped" from the fiber.

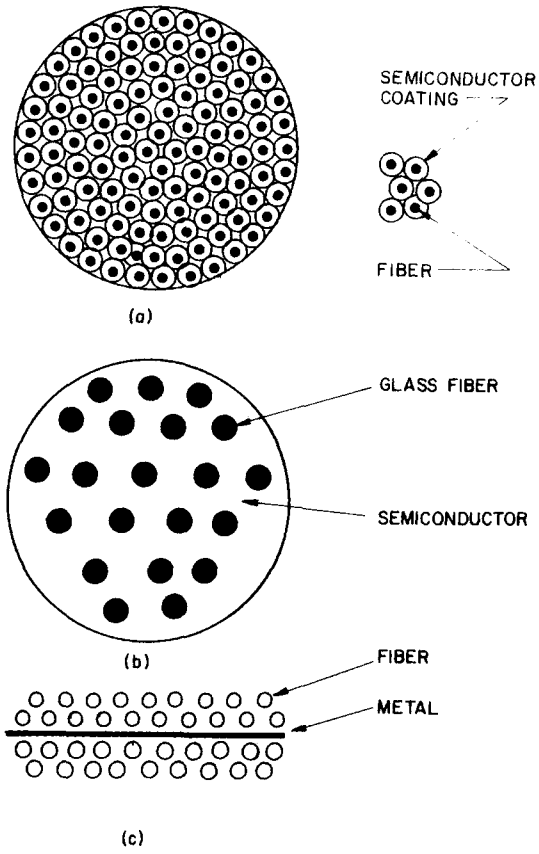

Figure 6. Fiber bundles: a) bundle of individually coated fibers, b) fibers embedded in a continuous semiconductor, c) fibers aligned parallel to metal conducting sheet.

5a, b or c, as appropriate. The potential loss for a fiber bundle is identical to that derived for the isolated fiber, provided that the average catalyst thickness per fiber remains the same.

If conducting wires, between and parallel to the fibers, are embedded in a semiporous semiconductor matrix, a radial potential drop between the fibers and the wire will exist. An exact analysis of the potential profile would require a complicated light intensity summation from the neighboring fibers. Instead, an order of magnitude estimate of the maximum radial potential drop to any wire is obtained here. The radial potential change is approximately

$$V = \frac{j}{\sigma} s \tag{22}$$

where s is a characteristic distance.

Typically s would be about half of the interfiber spacing d_b. The minimum conductivity is σ_o, the intrinsic semiconductor conductivity. The maximum current density is equal to the photon absorption rate for the n_f fibers in the bundle in a distance dz multiplied by χ and divided by the cross sectional area of the n_w wires in the bundle. The total intensity loss in an axial distance dz of the bundle is

$$\Delta I = n_f I_o \left(\exp\left(\frac{-z_1\phi}{L}\right) - \exp\left(\frac{-z_2\phi}{L}\right)\right) \simeq n_f I_o \cdot \frac{dz\phi}{L} \cdot e^{\frac{-z_1\phi}{L}}$$

The maximum current density is at $Z_1 = 0$:

$$j = \frac{\pi n_f I_o \frac{dz\phi}{L} \chi d_f^2}{4 m_w \pi d_w dz} \tag{23}$$

where d_w is the wire diameter. Substitution into Eq. 22 gives

$$V = \frac{n_f I_o \phi \chi d_b d_f^2}{8 m_w L d_w \sigma} \tag{24}$$

A calculation with typical parameters showed that this voltage drop is negligible (2×10^{-7} V).

NON-ISOTHERMAL PHOTO-ELECTRODE

A previous paper (Marinangeli and Ollis, 1980) showed that heat generation by light absorption may cause considerable temperature gradients for large fiber bundles or high intensities. Since electrical conductivity is a function of temperature (Kittel, 1971), the previous single fiber analysis may not apply to a non-isothermal fiber bundle. Photoconductivity also depends on temperature as the magnitudes of the various recombination routes depend on temperature (Simmons and Taylor, 1972). Since appreciable radial temperature gradients may occur in a bundle, a two dimensional potential profile will now exist.

In an efficient photo-electrode, the resistive heating will be small, and a portion of the photons, equal to the quantum yield, χ, will drive the chemical reaction. A fraction $\Delta H_{rxn}/E_g$ of this energy portion will be stored in the chemical reaction. In this case a simplified temperature profile may be used.

$$T/T_o = 1 + \left(1 - \frac{\chi \Delta H_{rxn}}{E_g}\right) \hat{F}(z) \left(1 - \left(\frac{R}{F_o}\right)^2\right) \tag{25}$$

where

$$\hat{F}(z) = \frac{R_v^2 \alpha_v I_o \beta_c' \exp(-z\phi/L) f d_f}{2 k_e T_o \epsilon d_c}$$

The temperature dependence of the conductivity for amorphous semiconductors is (Grigorovici, 1971)

$$\sigma = \sigma_o^* \exp\left(\frac{-E_g}{2kT}\right) \tag{26}$$

The Fermi level is near the middle of the band gap for most amorphous materials. For n or p type semiconductors

$$\sigma = \sigma_o^* \exp\left(\frac{-(E_c - E_F)}{kT}\right) \tag{26a}$$

The potential distribution may be obtained by solving the current balance for a cylindrical shell of the fiber bundle. We assume that the bundle radius is much greater than the radius of an individual fiber so that average properties of the bundle may be used. The conductivity will be non-isotropic, reflecting the non-isotropic (i.e., parallel) distribution of the insulating optical fibers.

A current blance on a cylindrical volume element yields

$$2\pi(R + \Delta R)\Delta z j_R|_{R+\Delta R} - 2\pi R \Delta z j_R|_R + 2\pi R \Delta R j_z|_{z+\Delta z} - 2\pi R \Delta R j_z|_z = \chi \alpha_c \bar{I}_c 2\pi R \cdot \Delta R \Delta z \tag{27}$$

The axial and radial current fluxes are j_z and j_R respectively. The light intensity has been averaged over the y direction for each individual fiber

$$\bar{I}_c = \frac{\int_0^{d_c} \beta_c I_o \exp\left(-\phi \frac{z}{L} - 2\frac{y}{d_p}\right) dy}{d_c} = \frac{\beta_c I_o}{2 d_c}\left(1 - \exp\left(\frac{-2d_c}{d_p}\right)\right) \exp\left(\frac{-z\phi}{L}\right) \tag{28}$$

The local current fluxes are given by Ohm's law

$$j_R = -\sigma_R \frac{\partial V}{\partial R}$$

$$j_z = -\sigma_z \frac{\partial V}{\partial z}$$

Substitution into Eq. 27 gives

$$\frac{\partial}{\partial R}\left(\sigma_R \frac{\partial V}{\partial R} + \frac{\sigma_R}{R}\frac{\partial}{\partial R}\right) + \frac{\partial}{\partial z}\left(\sigma_z \frac{\partial V}{\partial z}\right) = -\chi \alpha_c \bar{I}_c. \tag{29}$$

When heating by light absorption dominates, the temperature profile may be calculated first from Eq. 25. Then the conductivity at every point can be calculated (Eq. 26a). Finally, Equation 29 may be solved numerically.

Note that an increase in temperature will reduce the potential drop in the bundle. Too high a temperature may deactivate photo-assisted heterogeneous oxide catalyst for gaseous reactants (Formenti et al., 1971); this dependence for liquid-phase systems appears to be unexplored.

ACKNOWLEDGMENT

The authors thank the Energy Research and Development Agency and the National Science Foundation for support during this study. We are indebted to Prof. Peter Mark (deceased) for several useful criticisms of this paper.

NOTATION

a = cross-sectional area
A = concentration
A_o = concentration in the external phase
B = $\dfrac{\alpha_c \beta_c I_o \chi d_p L}{2 d_c \phi}\left(1 - e^{-2d_c/d_p}\right)$
C = s_o
D = $\dfrac{\sigma_o \alpha_c \beta_c I_o d_p}{2 n_o R' d_c}\left(1 - e^{-2d_c/d_p}\right)$
D_e = effective diffusivity
d_c = catalyst (semiconductor) thickness
d_f = fiber diameter
d_p = penetration depth of the evanescent wave
d_w = wire diameter
e = electronic charge
$\bar{E}$ = electric field
E_c = conduction band energy
E_F = Fermi level energy
E_g = energy band gap
E_{ox} = oxidation potential
E_{red} = reduction potential
E_v = valence band energy
f = catalyst (semiconductor) fraction in a fiber bundle
$\hat{F}$ = ratio of heat generation from light absorption to maximum heat conduction
i = current
I_c = light intensity in the catalyst (semiconductor)
$\bar{I}_c$ = average I_c
I_o = initial light intensity in the fiber
j = current density
k = Boltzmann's constant
k_e = thermal conductivity
ℓ = electron mean free path
L = fiber length
m_e = effective mass of an electron
m_w = effective mass of a hole
n = electron concentration
n_f = number of fibers
n_o = thermal equilibrium electron concentration
N = bundle Thiele modulus
N_{Pr} = Prater number
p = hole concentration
P = power
r = resistance
$\hat{r}$ = reaction rate
R = radial distance in the fiber bundle
R' = recombination rate
R_o = fiber bundle radius
s = characteristic distance
t = film thickness
T = Temperature
T_o = temperature in the external phase
u = $\exp(z\phi/L)$
v = volume
v_e = electron velocity
v_{th} = electron thermal velocity
V = voltage
V_b = magnitude of band bending (surface potential)
x = distance around a fiber perimeter
y = radial distance in the catalyst (semiconductor)
z = axial distance in the fiber of catalyst (semiconductor)
z^* = arbitrary z

Greek Letters

α_c = absorption coefficient of the catalyst (semiconductor)
β_c = ratio of light intensity inside and outside the fiber
ϵ = void fraction of a fiber bundle
μ = carrier mobility
μ_B = bulk carrier mobility
μ_e = electron mobility
μ_F = thin film mobility
μ_h = hole mobility
ϕ = characteristic decay length for light in a fiber
μ = conductivity
μ_o = intrinsic conductivity
μ_o^* = maximum intrinsic conductivity
σ_p = photo-conductivity contribution
σ_R = radial conductivity
σ_z = axial conductivity
τ = characteristic carrier collision time
χ = quantum efficiency

LITERATURE CITED

Adler, D., *Amorphous Semiconductors*, CRC Press, Cleveland (1971).

Albery, W., and M. Archer, "Photogalvanic Cells I. The Potential at Zero Current," *Electrochim. Acta*, **21**, 1155 (1976).

———, "Photogalvanic Cells II. Current-Voltage and Power Characteristics," *J. Electrochem. Soc.*, **124**, 688 (1977).

Archer, M. D., "Electrochemical Aspects of Solar Energy Conversion," *J. Appl. Electrochem.*, **5**, 17 (1975).

Becquerel, E., "Report on the Electrical Effects Produced under the Influence of Solar Radiation," *Comptes Rendus de L'academie des Sciences*, **9**, 561 (1939).

Bockris, J. O'M., and K. Uosaki, "The Theory of Hydrogen Production in a Photoelectrochemical Cell," Conference Proceedings, V. 2, First World Hydrogen Energy Conference, March 1976 Miami Beach, Florida, p. 5B-1 (1977).

Bolts, J. M., and M. S. Wrighton, "Correlation of Photocurrent-Voltage Curves with Flat-Band Potential for Stable Photoelectrolysis of Water," *J. Phys. Chem.*, **80**, 2641 (1976).

Born, M., and E. Wolf, *Principles of Optics 3rd Ed.*, Pergamon Press, Oxford (1965).

Bube, R. H., *Photoconductivity of Solids*, Wiley and Sons, New York (1960).

Butler, M. A., "Photoelectrolysis and Physical Properties of the Semiconducting Photoelectrode WO_3," *J. Appl. Phys.*, **48**, 1914 (1977).

Butler, M. A., R. D. Nasby, and R. K. Quinn, "Tungsten Trioxide as an Electrode for Photoelectrolysis of Water," *Solid State Comm.*, **19**, 1011 (1976).

Candea, R. M., M. Kasteur, R. Goodman, and N. Hickok, "Photoelectrolysis of Water: Silicon in Salt Water," *J. Appl. Phys.*, **47**, 2724 (1976).

Carey, J. H., and B. G. Oliver, "Intensity Effects in the Electrochemical Photolysis of Water at the Titanium Dioxide Electrode," *Nature*, **259**, 554 (1976).

Chai, Y. G., and W. W. Anderson, "Semiconductor Electrolyte Photovoltaic Cell Energy Conversion Efficiency," *Appl. Phys. Lett.*, **27**, 183 (1975).

Chang, C. C., A. Heller, B. Schwartz, S. Menezes, and B. Miller, "Stable Semiconductor Liquid Junction Cell with 9 Percent Solar-to-Electrical Conversion Efficiency," *Science*, **196**, 1097 (1977).

Chopra, K. L., *Thin Film Phenomena*, McGraw-Hill, New York (1969).

Ellis, A. B., S. W. Kaiser, and M. S. Wrighton, "Visible Light to Electrical Energy Conversion. Stable Cadmium Sulfide and Cadmium Selenide Photoelectrodes in Aqueous Electrolytes, *J. Amer. Chem. Soc.*, **98**, 1635 (1976a).

——, "Optical to Electrical Energy Conversion: Cadmium Telluride-Based Photoelectrochemical Cells Employing Telluride/Ditelluride Electrolytes," *ibid*, 6418 (1976b).
——, "Optical to Electrical Energy Conversion: Characterization of Cadmium Sulfide and Cadmium Selenide Based Photoelectrochemical Cells," *ibid.*, 6855 (1976c).
——, "Semiconducting Potassium Tantalate Electrodes. Photo-assistance Agents for the Efficient Electrolysis of Water," *J. Phys. Chem.*, **80,** 1325 (1976d).
Ellis, A. B., S. W. Kaiser, J. M. Bolts, and M. S. Wrighton, "Study of n-Type Semiconducting Cadmium Chalcogenide-Based Photoelectrochemical Cells Employing Polychalcogenide Electrolytes," *J. Amer. Chem. Soc.*, **99,** 2839 (1977a).
Ellis, A. B., J. M. Bolts, S. W. Kaiser, and M. S. Wrighton, "Study of n-Type Gallium Arsenide and Gallium Phosphide-Based Photoelectrochemical Cells. Stabilization by Kinetic Control and Conversion of Optical Energy to Electricity," *ibid*, 2848 (1977b).
Fleischauer, P. D., and J. K. Allen, "Photochemical Hydrogen Formation by Dye Sensitization of Titanium Dioxide Thin Film Electrodes," Aerospace Report No. ATR-76 (8208)-1, The Aerospace Corp., El Segundo, CA (1976).
Formenti, M., F. Juillet, P. Meriaudeau, and S. J. Teichner, "Heterogeneous Photocatalysis for Partial Oxidation of Paraffins," *Chem. Technol.*, **1,** 680 (1971).
Frank, S. N., and A. J. Bard, "Semiconductor Electrodes. II Electrochemistry of n-Type Titanium Dioxide Electrodes in Acetonitrile Solutions," *J. Amer. Chem. Soc.*, **97,** 7427 (1975).
Fujishima, A., and K. Honda, "Electrochemical Photolysis of Water at a Semiconductor Electrode," *Nature*, **238,** 37 (1972).
Fujishima, A., K. Kohayakawa, and K. Honda, "Hydrogen Production under Sunlight with an Electrochemical Photocell," *J. Electrochem. Soc.*, **122,** 1487 (1975).
Fujishima, A., T. Luase, and K. Honda, "Effect of Irradiation with Ultraviolet Light on the Spectral Sensitization of the Photoelectrochemical Process of a Zinc Oxide Single Crystal Electrode," *J. Amer. Chem. soc.*, **98,** 1625 (1976).
Gerischer, H., and K. Camman, "Photoelectrochemical Processes and Photocatalysis of Zinc Oxide Suspensions and Zinc Oxide Layers," *Ber. Bunsenges. Phys. Chem.*, **76,** 385 (1972).
——, "Electrochemical System for Water Photolysis Using Solar Energy," *ibid*, **80,** 1046 (1976).
Gerischer, H., "Electrochemical Photo and Solar Cells. Principles and Some Experiments," *J. Electroanal. Chem.*, **58,** 263 (1975).
Ginley, D. S., and M. A. Butler, "The Photoelectrolysis of Water Using Iron Titanate Anodes," *J. Appl. Phys.*, **48,** 2019 (1977).
Gissler, W. P., L. Lenski, and S. Pizzini, "Electrochemical Investigation of an Illuminated Titanium Dioxide Electrode," *J. Appl. Electrochem.*, **6,** 9 (1976).
Goetzberger, A., E. Clausmann, and M. J. Schultz, "Interface States on Semiconductor/Insulator Surfaces," *CRC Crit. Rev. Solid State Sci.*, **6,** 1 (1976).
Gourgaud, S., and D. Eliot, "Semiconductor/Electrolyte Photoelectric Energy Conversion: The Use of a Molybdenum Oxide Coating to Avoid Corrosion," *J. Electrochem. Soc.*, **124,** 102 (1977).
Grigorovici, R., "Amorphous Semiconducting Thin Films," *Thin Solid Films*, **9,** 1 (1971).
Haller, G. L., R. W. Rice, and Z. C. Wan, "Applications of Internal Reflection Spectroscopy to Surface Studies," *Catalysis Reviews*, **13,** 259 (1976).
Hardee, K. L., and A. J. Bard, "Semiconductor Electrodes. I The Chemical Vapor Deposition and Application of Polycrystalline n-Type Titanium Dioxide Electrodes to the Photosensitized Electrolysis of Water," *J. Electrochem. Soc.*, **122,** 739 (1975).
——, "Semiconductor Electrodes. V The Application of Chemically Vapor Deposited Iron Oxide Films to Photosensitized Electrolysis," *ibid*, **123,** 1024 (1976).
——, "Semiconductor Electrodes. X Photoelectrochemical Behavior of Several Polycrystalline Metal Oxide Electrodes in Aqueous Solution," *ibid*, 124, 215 (1977).
Harrick, N. J., *Internal Reflection Spectroscopy*, Interscience Publishers, New York (1967).
Harris, L. A. and R. H. Wilson, "Aging Effects in Single Crystal Reduced Rutile Anodes," *J. Electrochem. Soc.*, **123,** 1010 (1976).
Harris, L. A., D. R. Cross, and M. E. Gerstner, "Corrosion Suppression on Rutile Anodes by High Energy Redox Reactions," *J. Electrochem. Soc.*, **124,** 839 (1977).
Heller, A., K. C. Chang, and B. Miller, "Spectral Response and Efficiency Relations in Semiconductor Liquid Junction Solar Cells," *J. Electrochem. Soc.*, **124,** 697 (1977).
Hill, R. M., "Transport Phenomena in Thin Films," *Thin Solid Films*, **12,** 367 (1972).
Hodes, G., D. Cohen, and J. Manassen, "Tungsten Trioxide as a Photoanode for a Photoelectrochemical Cell," *Nature*, **260,** 312 (1976).
Hodes, G., J. Manassen, and D. Cohen, "Photoelectrochemical Energy Conversion and Storage Using Polycrystalline Chalcogenide Electrodes," *Nature*, **261,** 403 (1976).
Inoue, T., T. Watanabe, A. Fujishima, K. Honda, K. Kohayakawa, "Suppression of Surface Dissolution of CdS Photoanode by Reducing Agents," *J. Electrochem. Soc.*, **124,** 719 (1977).
Jayadeviah, T. S., "Semiconductor-Electrolyte Interface Devices for Solar Energy Conversion," *Appl. Phys. Lett.*, **25,** 399 (1974).
Keeney, J., D. H. Weinstein, and G. M. Haas, "Electricity from Photosensitization of Titanium," *Nature*, **253,** 719 (1975).
Kim, H., and H. Laitinen, "Photoeffects of Polycrystalline Tin Oxide Electrodes," *J. Electrochem. Soc.*, **122,** 53 (1975).
Kittel, C., *Introduction to Solid State Physics*, 4th ed., Wiley, New York (1971).
Kohl, P. A., S. N. Frank, and A. J. Bard, "Semiconductor Electrodes. XI Behavior of n and p type Semiconductors Covered with Thin n-TiO_2 Films," *J. Electrochem. Soc.*, **124,** 225 (1977).
Laser, D., and A. J. Bard, "Semiconductor Electrodes. VI A Photoelectrochemical Solar Cell Employing a Titanium Dioxide Anode and an Oxygen Cathode," *J. Electrochem. Soc.*, **123,** 1027 (1976).
Manassen, J., D. Cohen, G. Hodes, and A. Sofer, "Electrochemical, Solid State, Photochemical and Technological Aspects of Photochemical Energy Converters," *Nature*, **263,** 97 (1976).
Manassen, J., G. Hodes, and D. Cohen, "Photoelectrochemical Energy Conversion and Storage. The Polycrystalline Cadmium Sulfide Cell with Different Storage Modes," *J. Electrochem. Soc.*, **124,** 532 (1977).
Mavroides, J. G., D. I. Tchernev, J. A. Kafalas, and D. F. Kolesar, "Photoelectrolysis of Water in Cells with Titanium Dioxide Anodes," *Materials Res. Bull.*, **10,** 1023 (1975).
Mavroides, J. G., J. A. Kafolas, and D. F. Kolesor, "Photoelectrolysis of Water in Cells with Strontium Titanate Anodes," *Appl. Phys. Lett.*, **28,** 241 (1976).
Marianageli, R. E., and D. F. Ollis, "Photoassisted Heterogeneous Catalysis with Optical Fibers. I Isolated Single Fiber," *AIChE J. 22* (1977).
——, "Photoassisted Heterogeneous Catalysis with Optical Fibers. II Non-isothermal Single Fiber and Fiber Bundle," *AIChE J.* **26,** 1000 (1980).
Mark, P., and B. Sang Lee, "Current Voltage Dependencies of Heterogeneous Semiconductor Systems," *J. Phys. Chem. Solids*, **35,** 865 (1974).
Miller, B., and A. Heller, "Semiconductor Liquid Junction Solar Cells Based on Anodic Sulfide Films," *Nature*, **262,** 680 (1976).
Morisaki, H., T. Watanabe, M. Luase, and K. Yazawa, "Photoelectrolysis of Water with Titanium Dioxide-Covered Solar Cell Electrodes," *Appl. Phys. Lett.*, **29,** 338 (1976).
Morrison, S. R., *The Chemical Physics of Surfaces*, Plenum Press, New York (1977).
Nakato, Y., T. Ohnishi, and H. Tsubomura, "Photoelectrochemical Behavior of Semiconductor Electrodes Coated with Thin Metal Films," *Chem. Lett.*, 883 (1975).
Nakato, Y., K. Abe, and H. Tsubomura, "A New Photovoltaic Effect Observed for Metal-Coated Semiconductor Electrodes and its Utilization for the Photolysis of Water," *Ber. Brunsenges. Phys. Chem.*, **80,** 1002 (1976).
Nasby, R. D., and R. K. Quinn, "Photoassisted Electrolysis of Water Using a Barium Titanate Electrode," *Materials Res. Bull.*, **11,** 985 (1976).
Nozik, A. J., "Photoelectrolysis of Water Using Semiconducting Titanium Dioxide Crystals," *Nature*, **257,** 383 (1975).
——, "Energy Conversion via Photoelectrolysis," Proceedings 11th Intersociety Energy Conversion Engineering Conference, **1,** 43 (Sept., 1976a).
——, "P-N Photoelectrolysis Cells," *Appl. Phys. Lett.*, **29,** 150 (1976b).
——, "Photochemical Diodes," *Appl. Phys. Lett.*, **30,** 567 (1977).
Ohnishi, T., Y. Nakato, and H. Tsubomura, "The Quantum Yield of Photolysis of Water on Titanium Dioxide Electrodes," *Ber. Bunsenges Phys. Chem.*, **79,** 523 (1975).
Ohashi, K., J. McCann, and J. O'M. Bockris, "Stable Photoelectrochemical Cells for the Splitting of Water," *Nature*, **266,** 611 (1977).
Owen, J. R., "A Proposed Cadmium-Selenium Film-Electrolyte Schottky Barrier Solar Cell," *Nature*, **267,** 504 (1977).
Quinn, R. K., R. D. Nasby, and R. J. Baughman, "Photoassisted Electrolysis of Water Using Single Crystal Alpha-Iron Oxide (α Fe_2O_3) Anodes," *Materials Res. Bull.*, **11,** 1011 (1976).
Simmons, J. G., and G. W. Taylor, "Theory of Steady State Photoconduc-

tivity in Amorphous Semiconductors," *J. Non-Crystalline Solids*, **8–10**, 947 (1972).
Spitler, M. T., and M. Calvin, "Electron Transfer at Sensitized TiO_2 Electrodes," *J. Chem. Phys.*, **66**, 4294 (1977).
Takahashi, F., and R. Kikuchi, "Photoelectrolysis Using Chlorophyll Electrodes," *Biochim. Biophys. Acta*, **430**, 490 (1976).
Taylor, G. W., and J. G. Simmons, "Basic Equations for Statistics, Recombination Processes, and Photoconductivity in Amorphous Insulators and Conductors," *J. Non-Crystalline Solids*, **8–10**, 940 (1972).
Tomkiewicz, M., and J. M. Woodall, "Photoassisted Electrolysis of Water by Visible Irradiation of a p-type Gallium Phosphide Electrode," *Science*, **196**, 990 (1977).
Tributsch, H., "Layer-Type Transition Metal Dichalcogenides—A New Class of Electrodes for Electrochemical Solar Cells," *Ber. Bunsenges. Phys. Chem.*, **81**, 361 (1977).
van Roosbroeck, W., "The Transport of Added Current Carriers in a Homogeneous Semiconductor," *Phys. Rev.*, **91**, 282 (1953).
Wrighton, M. S., D. S. Ginley, P. T. Wolczanski, A. B. Ellis, D. L. Morse, and A. Linz, "Photoassisted Electrolysis of Water by Irradiation of a Titanium Dioxide Electrode," *Proc. Nat. Acad. Sci. USA*, **72**, 1518 (1975).
Wrighton, M. S., D. L. Morse, A. B. Ellis, D. S. Ginley, and H. B. Abrahamson, "Photoassisted Electrolysis of Water by Ultraviolet Irradiation of an Antimony Doped Stannic Oxide Electrode," *J. Amer. Chem. Soc.*, **98**, 44 (1976a).
Wrighton, M. S., A. B. Ellis, P. T. Wolczanski, D. L. Morse, H. B. Abrahamson, and D. S. Ginley, "Strontium Titanate Photoelectrodes. Efficient Photoassisted Eletrolysis of Water at Zero Applied Potential," *ibid*, 2774 (1976b).
Wrighton, M. S., J. M. Bolts, A. B. Ellis, and S. W. Kaiser, "Photoassisted Electrolysis of Water: Conversion of Optical to Chemical Energy," Proceedings—11th Intersociety Energy Conversion Engineering Conference, **1**, 35 (Sept., 1976c).
Yeh, L. R., and N. Hackerman, "Iron Oxide Semiconductor Electrodes in Photoassisted Electrolysis of Water," *J. Electrochem. Soc.*, **124**, 833 (1977).
Yoneyama, H., H. Sakamoto, and H. Tamura, "A Photo-electrochemical Cell with Production of Hydrogen and Oxygen by a Cell Reaction," *Electrochim. Acta* **20**, 341 (1975).

Manuscript received February 1, 1978; revision received October 16, and accepted October 24, 1980.

Effects of London-van der Waals Forces on the Thinning of a Dimpled Liquid Film As a Small Drop or Bubble Approaches a Horizontal Solid Plane

When a small drop or bubble approaches a solid surface, a thin liquid film forms between them, drains, until an instability forms and coalescence occurs. Lin and Slattery (1982a) developed a hydrodynamic theory for the first portion of this coalescence process: the drainage of the thin liquid film while it is sufficiently thick that the effects of London-van der Waals forces and electrostatic forces can be ignored. Here the effects of the London-van der Waals forces are included. The resulting theory describes the evolution of the film profile, given only the bubble radius and the required physical properties. The inclusion of a positive disjoining pressure results in better descriptions of the film profiles measured by Platikanov (1964) for air bubbles pressed against glass plates. When the disjoining pressure is negative, an unstable draining film evolves and finally ruptures. Unfortunately, there are no experimental data with which to compare our predicted coalescence times.

JING-DEN CHEN and J. C. SLATTERY

Department of Chemical Engineering
Northwestern University
Evanston, IL 60201

SCOPE

The rate at which drops or bubbles suspended in a liquid coalesce is important to the preparation and stability of emulsions, of foams, and of dispersions; to liquid-liquid extraction; to the formation of an oil bank during the displacement of oil from a reservoir rock. On a smaller scale, when two drops (bubbles) in a liquid phase approach each other or when a drop (bubble) approaches a solid surface, a thin liquid film forms between them, drains, until an instability forms and coalescence occurs. We must understand the factors controlling the rate of coalescence.

Lin and Slattery (1982a,b) considered the early stage of this coalescence process as a drop approaches a solid wall or a fluid-fluid interface. Their results are applicable, when the draining film is sufficiently thick that effects of any electrostatic double layer or of London-van der Waals forces can be neglected.

In what follows, we extend their theory to include the effects of London-van der Waals forces on the drainage process. In order to simplify the problem, we consider only the case of small drops or bubbles approaching a horizontal solid wall. The liquid films are so thin that the Reynolds lubrication theory approximation can be applied.